A micro-macro decomposition based asymptotic-preserving scheme for the multispecies Boltzmann equation*

Shi Jin† Yingzhe Shi‡

Abstract

In this paper we extend the micro-macro decomposition based asymptotic-preserving scheme developed in [3] for the single species Boltzmann equation to the multispecies problems. An asymptotic-preserving scheme for kinetic equation is very efficient in the fluid regime where the Knudsen number is small and the collision term becomes stiff. It allows coarse (independent of Knudsen number) mesh size and large time step in the fluid regime. The difficulty associated with multispecies problems is that there are no local conservation laws for each species, resulting in extra stiff nonlinear source terms that need to be discretized properly in order to 1) avoid Newton type solvers for nonlinear algebraic systems and 2) to be asymptotic-preserving. We show that these extra nonlinear source terms can be solved using only linear system solvers, and the scheme preserves the correct Euler and Navier-Stokes limits. Numerical examples are used to demonstrate the efficiency and applicability of the schemes for both Euler and Navier-Stokes regimes.

Keywords: multispecies Boltzmann equation, BGK model, micro-macro decomposition, asymptotic-preserving scheme, fluid dynamic limit

AMS subject classifications.: 65M06, 82C40, 82C80, 41A60, 76P05

1 Introduction

In kinetic theory, the Boltzmann equation is a fundamental equation to describe the evolution of rarefied gases. In this paper, we are interested in the multispecies Boltzmann equation for the gas mixture. Such equations arise in many applications. One example is the atmosphere which must be considered at least as the mixture of Oxygen and Nitrogen. Other applications of the gas mixture include the problems in evaporation-condensation or in the nuclear engineering.

Typical computational challenges for the Boltzmann equation include its high dimensionality, and the existence of multiscale where the Knudsen number–the ratio of the mean free path over a typical length scale such as the domain size–can have different order of magnitude in different part of the domain. When the Knudsen number is small, the solution to the Boltzmann equation can be approximated by the compressible Euler or Navier-Stokes equations via the Chapman-Enskog expansion [9]. This is the so-called fluid dynamic regime, which is known to be numerical stiff due to the stiff collision term. Our aim is to develop numerical schemes for the multispecies Boltzmann equation that are efficient in the fluid dynamic regime, namely we are seeking numerical schemes that can allow macroscopic (or fluid dynamic) mesh size and time step.

The asymptotic-preserving (AP) methods are a general framework for kinetic equations with different scales of the Knudsen number. According to Jin [13], a scheme for kinetic equation is AP if

- it preserves the discrete analogy of the Chapman-Enskog expansion, namely, it is a suitable scheme for the kinetic equation, yet, when holding the mesh size and time step fixed and letting the Knudsen number go to zero, the scheme becomes a suitable scheme for the limiting Euler equations

*This work was partially supported by NSF grant No. DMS-0608720 and NSF FRG grant DMS-0757285. SJ was also supported by a Van Vleck Distinguished Research Prize from University of Wisconsin-Madison.

†Department of Mathematics, University of Wisconsin, Madison, WI 53706, USA (jin@math.wisc.edu)

‡Department of Mathematics, University of Wisconsin, Madison, WI 53706, USA (shi@math.wisc.edu)

- implicit collision terms can be implemented explicitly, or at least more efficiently than using the Newton type solvers for nonlinear algebraic systems.

Comparing with a multiphysics domain decomposition type method [4, 6, 7, 12, 18, 24], the AP schemes avoid the coupling of physical equations of different scales where the coupling conditions are difficult to obtain, and interface locations hard to determine. The AP schemes are based on solving one equation– the kinetic equation, and they become a robust macroscopic (fluid) solver *automatically* when the Knudsen number goes to zero. An AP scheme implying a numerical convergence uniformly in the Knudsen number was proved by Golse-Jin-Levermore for linear transport equation in the diffusion regime [10]. This result can be extended to essentially all AP schemes, although the specific proof is problem dependent. For examples of AP schemes for kinetic equations in the fluid dynamic or diffusive regimes see for examples [5, 15, 16, 17, 11].

An AP scheme for (single species) Boltzmann equation was introduced by Benoune, Lemou and Mieussens [3] using the micro-macro decomposition of the Boltzmann equation. The micro-macro decomposition writes the density distribution function as the sum of the local Maxwellian and the non-thermoequalibrium deviator. A coupled system for the hydrodynamic moments (density, momentum and total energy) and the deviator can be formed which recovers both Euler and Navier-Stokes equations via the Chapman-Enskog expansion. It has found theoretical success [21], and has also been used for numerical purposes, see [8, 19]. It was shown in [8] that a AP scheme can be constructed by using the micro-macro decomposition of the Boltzmann equation. The scheme is AP in the Euler limit. By suitably resolving the viscous term it is also consistent to the Navier-Stokes approximation. It is our goal to extend this scheme to multispecies Boltzmann equation.

For multispecies Boltzmann equation, each species does not conserve the momentum and energy, although these quantities for the entire systems are conserved. This feature brings new difficulty for numerical approximations not encountered in the single species case. The non-conservation of each species introduces stiff nonlinear source terms that must be discretized with care in order 1) to be AP and 2) to be solved efficiently by avoiding the iterative Newton solvers for nonlinear algebraic systems. Our discretizations are designed to satisfy these two properties, as will be shown asymptotically and demonstrated numerically.

For convenience and clarity we will mostly use the simpler multispecies BGK model introduced in [1], yet for completeness and generality we will also present the framework for the general Boltzmann equation.

The paper is organized as follows. In Section 2, we briefly review the multispecies Boltzmann equation. We then introduce the consistent BGK model for gas mixtures and its hydrodynamic limits of Euler and Navier-Stokes equations. In Section 3, we present the micro-macro decomposition method, and use it to construct the equivalent kinetic/fluid system to the Boltzmann equation. This system is proved to have the Euler and Navier-Stokes limits via the Chapman-Enskog expansion. Section 4 gives the detailed numerical approximations based on the kinetic/fluid coupling system. We show that it is AP to the Euler limit, and is also consistent to the Navier-Stokes approximation for suitably small mesh size and time step. We also show how the implicit nonlinear source term can be solved via only *linear* system solvers. In Section 5, some numerical tests are conducted to validate our model and the schemes. We make some concluding remarks in section 6.

2 Multispecies models

2.1 The multispecies Boltzmann equation

The Boltzmann equation describes the density distribution of evolution of rarefied gases. For the mixtures, the Boltzmann equation (refer to [9]) is written as

$$\partial_t f_i + \xi \cdot \nabla_x f_i = \frac{1}{\epsilon} Q_i(f, f), \qquad t \geqslant 0, \quad (x, \xi) \in \mathbb{R}^d \times \mathbb{R}^d. \tag{1}$$

$f_i = f_i(t, x, \xi)$ represents the density distribution function of species-i particles that have position x and velocity ξ at time t; ϵ is the dimensionless Knudsen number, the mean free path over a typical length scale;

d is the space dimension. The collision term Q_i is defined by

$$Q_i(f,f) = \sum_{k=1} Q_{ik}(f_i, f_k),$$
$$Q_{ik}(f_i, f_k) = \int_{\mathbb{R}^d} \int_{B_+} (f_i' f_{k^*}' - f_i f_{k^*}) B_{ik}(\Omega \cdot V, |V|) d\xi_* d\Omega$$

where $B_{ik}(\Omega \cdot V, |V|)$ is the collision kernel; ξ and ξ_* are the molecular pre-collisional velocities; $\xi^{'}$ and ξ_*' are the post-collisional velocities; $f_i' = f_i'(t, x, \xi^{'})$, $f_{k^*}' = f_k(t, x, \xi_*')$, $f_{k^*} = f_k(t, x, \xi_*)$; Ω is an unit vector, B_+ is the semi-sphere defined by $\Omega \cdot V = 0$, V is the relative velocity

$$V = \xi - \xi_*.$$

We consider the elastic collisions of two particles: one from species i and the other from species k. Thus, the post-collisional velocities are

$$\begin{cases} \xi^{'} = \xi - \frac{2\mu_{ik}}{m_i} \Omega[(\xi - \xi_*) \cdot \Omega], \\ \xi_*^{'} = \xi_* + \frac{2\mu_{ik}}{m_k} \Omega[(\xi - \xi_*) \cdot \Omega]. \end{cases}$$

the mass of species i is m_i and the reduced mass is $\mu_{ik} = m_i m_k/(m_i + m_k)$. These velocity relations arise from the conservation laws for the momentum and energy in the molecules' collision

$$m_i \xi + m_k \xi_* = m_i \xi^{'} + m_k \xi_*^{'}$$
$$m_i |\xi|^2 + m_k |\xi_*|^2 = m_i |\xi^{'}|^2 + m_k |\xi_*^{'}|^2$$

If we define the microscopic collision operator

$$\Upsilon : (\xi, \xi_*) \mapsto (\xi^{'}, \xi_*^{'}),$$

the collision is reversible and satisfies

$$\Upsilon \circ \Upsilon = I$$

This property gives the following identities:

$$\begin{cases} d\xi d\xi_* = d\xi^{'} d\xi_*^{'} \\ (\xi - \xi_*) \cdot \Omega = -(\xi^{'} - \xi_*^{'}) \cdot \Omega \\ |\xi - \xi_*| = |\xi^{'} - \xi_*^{'}|. \end{cases}$$

2.2 Macroscopic quantities

We introduce the notations for macroscopic quantities of each species (i): n_i is the number density, ρ_i the mass density, u_i the average velocity, E_i the total energy, e_i the internal energy per particle, T_i the temperature, given by

$$n_i = \int f_i d\xi, \quad \rho_i = m_i \int f_i d\xi,$$
$$\rho_i u_i = m_i \int f_i \xi d\xi,$$
$$E_i = \frac{1}{2} \rho_i u_i^2 + n_i e_i = m_i \int f_i \frac{1}{2} |\xi|^2 d\xi,$$
$$e_i = \frac{d}{2} T_i = \frac{m_i}{2 n_i} \int f_i |\xi - u_i|^2 d\xi.$$

We also define global quantities for the mixture: the total mass density ρ, the number density n, the mean velocity u, the total energy E, the internal energy ne, and the mean temperature $T = \frac{2e}{d}$:

$$\begin{aligned}\rho &= \sum_i \rho_i, \quad n = \sum_i n_i,\\ \rho u &= \sum_i \rho_i u_i,\\ E &= \frac{d}{2}nT + \frac{\rho}{2}|u|^2 = \sum_i E_i.\end{aligned}$$

2.3 Properties of the Boltzmann equation

We use the notation in the following:

$$\langle\varphi\rangle = \int \varphi d\xi \quad \text{and} \quad H = (1, \xi, \frac{|\xi|^2}{2}).$$

The macroscopic quantities come from the moments of density distribution function

$$U_i = \langle m_i H f_i\rangle = \left(\rho_i, \rho_i u_i, \frac{1}{2}(\rho_i|u_i|^2 + dn_i T_i)\right).$$

The collision term Q_i satisfies the conservation laws of mass, the total momentum and the total energy

$$\begin{cases} \langle m_i Q_i\rangle = 0,\\ \sum_i \langle m_i \xi Q_i\rangle = 0,\\ \sum_i \langle m_i \frac{1}{2}|\xi|^2 Q_i\rangle = 0.\end{cases} \tag{2}$$

Moreover, the H-theorem holds:

$$\sum_i \langle m_i Q_i \log f_i\rangle \le 0 \qquad \text{for any } f_i > 0,$$

the "=" is satisfied at the equilibrium, which implies $Q_i(f, f) = 0$ $(\forall i)$ and f_i is the local Maxwellian

$$f_i = \overline{M_i}(U) = n_i(\frac{m_i}{2\pi T})^{d/2}\exp(-\frac{m_i|\xi - u|^2}{2T}) \tag{3}$$

where $u_i = u_k = u$, $T_i = T_k = T$ for any i and k (see [9]).

2.4 The multispecies BGK model

Consider the consistent BGK model introduced in [1] for the Maxwell molecules

$$\frac{df_i}{dt} = \partial_t f_i + \xi\cdot\nabla_x f_i = \frac{1}{\epsilon}Q_i := \frac{\nu_i}{\epsilon}(\widetilde{M_i} - f_i) \tag{4}$$

ν_i is the collision frequency defined as $\nu_i = \sum_k n_k\chi_{ik}$; χ_{ik} is the interaction coefficient

$$\chi_{ik} = \int_{B_+} (\cos\omega)^2 B_{ik}(\omega)d\omega$$

with the collision angle $\omega = \Omega\cdot V/|V|$; and

$$\widetilde{M_i} = n_i(\frac{m_i}{2\pi\widetilde{T_i}})^{d/2}\exp(-\frac{m_i|\xi - \widetilde{u_i}|^2}{2\widetilde{T_i}})$$

is a Maxwellian distribution with $\widetilde{u_i}$ and $\widetilde{T_i}$ defined below.

For the Maxwell molecule, the collision kernel $B_{ik}(\Omega \cdot V, |V|)$ is only related with the collision angle ω between the relative velocity V and unit vector Ω

$$B_{ik}(\Omega \cdot V, |V|) = B_{ik}(\omega).$$

Thus, the moments of the collision operator can be obtained as

$$\langle m_i Q_i \rangle = 0, \tag{5}$$

$$\langle m_i \xi Q_i \rangle = \nu_i \rho_i (\widetilde{u_i} - u_i) = \sum_k 2\mu_{ik}\chi_{ik} n_i n_k [u_k - u_i], \tag{6}$$

$$\langle m_i \frac{1}{2}|\xi|^2 Q_i \rangle = \nu_i (\widetilde{E_i} - E_i) = \sum_k 2\mu_{ik}\chi_{ik} n_i n_k \left[(u_k - u_i)u_i + \frac{2}{m_i + m_k} \left(e_k - e_i + m_k \frac{|u_k - u_i|^2}{2} \right) \right]. \tag{7}$$

Note that the momentum and energy are not conserved for each species.

From (5)-(7), the $\widetilde{u_i}$ and $\widetilde{T_i}$ in $\widetilde{M_i}$ have the expression ($\widetilde{e_i} = \frac{d}{2}\widetilde{T_i}$):

$$m_i \nu_i \widetilde{u_i} = m_i \nu_i u_i + \sum_k 2\mu_{ik}\chi_{ik} n_k (u_k - u_i), \tag{8}$$

$$\nu_i \widetilde{e_i} = \nu_i e_i - \frac{m_i \nu_i}{2} |\widetilde{u_i} - u_i|^2 + \sum_k 2\mu_{ik}\chi_{ik} n_k \frac{2}{m_i + m_k} \cdot \left(e_k - e_i + m_k \frac{|u_k - u_i|^2}{2} \right). \tag{9}$$

Taking moments on the BGK model (4), (5)-(7) gives the macroscopic equations:

$$\begin{cases} \partial_t \rho_i + \nabla_x \cdot (\rho_i u_i) = 0, \\ \partial_t \rho_i u_i + \nabla_x \cdot (\rho_i u_i \otimes u_i + P_i) = \frac{1}{\epsilon} \sum\limits_k 2\mu_{ik}\chi_{ik} n_i n_k [u_k - u_i], \\ \partial_t E_i + \nabla_x \cdot (E_i u_i + P_i u_i + q_i) = \frac{1}{\epsilon} \sum\limits_k 2\mu_{ik}\chi_{ik} n_i n_k \left[(u_k - u_i) \cdot u_i + \frac{2}{m_i + m_k} \left(e_k - e_i + m_k \frac{|u_k - u_i|^2}{2} \right) \right], \end{cases} \tag{10}$$

where P_i is a $d \times d$ stress tensor; q_i is the heat flux of species i.

It was shown in [1] that the BGK model possesses the following properties:

- the non-negativity of densities
- the exchange relations of momentum and energy complies with those of the Maxwell particles
- the indifferentiability principle holds: when all species are the same (the same mass and all $\chi_{ik} \equiv \chi$, $\forall i, k$), the model will degenerate into the single species BGK model
- the equilibrium distributions are local Maxwellians as (3) with mean velocity u and mean temperature T
- the H theorem holds true.

2.5 The fluid dynamics approximations of the multispecies BGK model

At the zero Knudsen number limit ($\epsilon \to 0$), all $Q_i = 0$. From (8) - (9), we have $\widetilde{u_i} = u_i = u$ and $\widetilde{T_i} = T_i = T$ (see [1]). Thus,

$$f_i = \overline{M_i} = n_i \left(\frac{m_i}{2\pi T}\right)^{d/2} \exp\left(-\frac{m_i |\xi - u|^2}{2T}\right),$$

and the macroscopic equations (10) become the Euler system

$$\begin{aligned} \partial_t \rho_i + \nabla_x \cdot (\rho_i u) &= 0, \\ \partial_t \rho u + \nabla_x \cdot (\rho u \otimes u + nT\bar{\bar{I}}) &= 0, \\ \partial_t E + \nabla_x \cdot ((E + nT)u) &= 0, \end{aligned}$$

with the pressure $P = nT\bar{\bar{I}}$, where $\bar{\bar{I}}$ is the unit matrix, and the heat flux $q = 0$.

When $\epsilon \ll 1$, the Chapman-Enskog expansion was used in [1] to get the Navier-Stokes equation as

$$\begin{aligned} \partial_t \rho_i + \nabla_x \cdot (\rho_i u) &= -\nabla_x \cdot (J_i), \\ \partial_t (\rho u) + \nabla_x \cdot (\rho u \otimes u + P) &= 0, \\ \partial_t E + \nabla_x \cdot [(E + P)u + q] &= 0, \end{aligned} \tag{11}$$

with

$$\begin{aligned} J_i &= \rho_i (u_i - u), \\ P &= nT\bar{\bar{I}} - \eta \left(\nabla_x u + (\nabla_x u)^T - \frac{2}{d} (\nabla_x \cdot u) \bar{\bar{I}} \right), \\ q &= \frac{d+2}{2} T \sum_i n_i (u_i - u) - \kappa \nabla_x T, \end{aligned} \tag{12}$$

where the viscosity coefficient $\eta = \epsilon T \sum_i \frac{n_i}{\nu_i}$, the thermal conductivity coefficients $\kappa = \epsilon \frac{d+2}{2} T \sum_i \frac{n_i}{m_i \nu_i}$, and J_i is the diffusion velocity

$$J_i = -\epsilon \sum_k L_{ik} \frac{\nabla_x (n_k T)}{\rho_k} + O(\epsilon^2),$$

in which L_{ik} is a symmetric matrix depending only on the densities.

3 A kinetic/fluid formulation

3.1 Micro/Macro decomposition

For each species i, as was done is [21, 3], we decompose the distribution function $f_i = f_i(t, x, \xi)$ into the sum of its Maxwellian $M_i(U_i)$ and $g_i = \frac{f_i - M_i}{\epsilon}$

$$f_i = M_i(U_i) + \epsilon g_i, \tag{13}$$

where the Maxwellian is

$$M_i(U_i) = n_i \left(\frac{m_i}{2\pi T_i} \right)^{d/2} \exp \left(-\frac{m_i |\xi - u_i|^2}{2T_i} \right). \tag{14}$$

The Maxwellian for species i has the same moments as the density distribution function f_i

$$\langle H f_i \rangle = \langle H M_i \rangle \tag{15}$$

thus,

$$\langle H g_i \rangle = 0.$$

One can use a projection method to separate the macroscopic and microscopic quantities M_i and g_i. Consider the Hilbert space $L^2_{M_i} = \left\{ \varphi | \quad \varphi \left(\frac{M_i}{n_i} \right)^{-\frac{1}{2}} \in L^2(\mathbb{R}^d) \right\}$, the scalar product $(\varphi, \psi)_{M_i} = \left\langle \varphi \psi \left(\frac{M_i}{n_i} \right)^{-1} \right\rangle$.

Define the space $D_{M_i} = \text{Span}\{M_i, \xi M_i, |\xi|^2 M_i\}$, then the orthogonal basis of D_{M_i} is

$$B = \left\{ \frac{M_i}{n_i}, \frac{\xi - u_i}{\sqrt{T_i/m_i}} \frac{M_i}{n_i}, \left(\frac{|\xi - u_i|^2}{2T_i/m_i} - \frac{d}{2} \right) \frac{M_i}{n_i} \right\},$$

and the orthogonal projection in $L^2_{M_i}$ onto D_{M_i} is $\Pi_{M_i}(\varphi)$:

$$\Pi_{M_i}(\varphi) = \frac{1}{n_i} \left[\langle \varphi \rangle + \frac{(\xi - u_i) \cdot \langle (\xi - u_i) \varphi \rangle}{T_i/m_i} + \left(\frac{|\xi - u_i|^2}{2T_i/m_i} - \frac{d}{2} \right) \frac{2}{d} \left\langle \left(\frac{|\xi - u_i|^2}{2T_i/m_i} - \frac{d}{2} \right) \varphi \right\rangle \right] M_i.$$

One can establish the following properties of $\Pi_{M_i}(\varphi)$ as in [3]:

Lemma 1. *As the definition of M_i and g_i in (13)(14), we have*

$$(I - \Pi_{M_i})(\partial_t M_i) = \Pi_{M_i}(g_i) = \Pi_{M_i}(\partial_t g_i) = 0.$$

Proof. We know that

$$\partial_t M_i = \left[\frac{\partial_t \rho_i}{\rho_i} + \frac{m_i(\xi - u_i)}{T_i} \cdot \partial_t u_i + \left(\frac{m_i |\xi - u_i|^2}{2T_i} - \frac{d}{2} \right) \frac{\partial_t T_i}{T_i} \right] M_i$$

clearly belongs to D_{M_i}. Thus, $\Pi_{M_i}(\partial_t M_i) = \partial_t M_i$. Since $\langle H g_i \rangle = 0$, $\langle H \partial_t g_i \rangle = \partial_t \langle H g_i \rangle = 0$. So it implies $\Pi_{M_i}(g_i) = \Pi_{M_i}(\partial_t g_i) = 0$. □

Now apply the operator $(I - \Pi_{M_i})$ to (1),

$$(I - \Pi_{M_i}) (\partial_t M_i + \xi \cdot \nabla_x M_i) + \epsilon (I - \Pi_{M_i}) (\partial_t g_i + \xi \cdot \nabla_x g_i) = \frac{1}{\epsilon} (I - \Pi_{M_i}) Q_i.$$

Using Lemma 1 one obtains:

$$\partial_t g_i + (I - \Pi_{M_i})(\xi \cdot \nabla_x g_i) = \frac{1}{\epsilon} \left[\frac{1}{\epsilon} (I - \Pi_{M_i}) Q_i - (I - \Pi_{M_i})(\xi \cdot \nabla_x M_i) \right]. \tag{16}$$

Taking the moments of (1), it gives:

$$\partial_t \langle m_i H M_i \rangle + \nabla_x \cdot \langle m_i \xi H M_i \rangle + \epsilon \nabla_x \cdot \langle m_i \xi H g_i \rangle = \frac{1}{\epsilon} \langle m_i H Q_i \rangle.$$

The macroscopic quantities U_i are defined as $\langle m_i H M_i \rangle$. Let $F(U_i) = \langle m_i \xi H M_i \rangle$ be the flux vector of U_i. Then, The equations for macroscopic quantities are

$$\partial_t U_i + \nabla_x \cdot F(U_i) + \epsilon \nabla_x \cdot \langle m_i \xi H g_i \rangle = \frac{1}{\epsilon} \langle m_i H Q_i \rangle. \tag{17}$$

The coupled system (16)-(17) gives a kinetic/fluid formulation of the multispecies Boltzmann equation. Next we will show that the system is equivalent to the Boltzmann equation (1), which essentially follows the proof in [3].

Proposition 2. *(i) Let f_i be a classical solution of the Boltzmann equation (1) with initial data $f_i(t = 0, x, \xi) = f_0(x, \xi)$, and $M_i = M_i(U_i)$ its associated Maxwellian given in (14). Then the pair (U_i, g_i), where $U_i = \langle m_i H M_i \rangle$ and $g_i = \frac{f_i - M_i}{\epsilon}$, is a solution to the coupled system (16)-(17) with the corresponding initial data*

$$U(t = 0) = U_0 = \langle m_i H f_{i0} \rangle \text{ and } g_i(t = 0) = g_{i0} = \frac{f_{i0} - M_{i0}}{\epsilon}. \tag{18}$$

(ii) Conversely, if (U_i, g_i) satisfies system (16)-(17) with the initial data (18) such that $\langle m_i H g_{i0} \rangle = 0$, then $f_i = M_i + \epsilon g_i$ is a solution to the Boltzmann equation (1) with initial data $f_{i0} = M_i(U_{i0}) + \epsilon g_{i0}$ and we have $U_i = \langle m_i H f_i \rangle$ and $\langle m_i H g_i \rangle = 0$.

Proof. (i) is straightforward due to the construction of the coupled system (16)-(17). Consider (ii), we have from (16)

$$\epsilon \partial_t g_i + \xi \cdot \nabla_x M_i + \epsilon \xi \cdot \nabla_x g_i = \frac{1}{\epsilon} (I - \Pi_{M_i}) Q_i + \Pi_{M_i}(\xi \cdot \nabla_x M_i) + \epsilon \Pi_{M_i}(\xi \cdot \nabla_x g_i).$$

Adding $\partial_t M_i$ to the above equations gives,

$$\partial_t f_i + \xi \cdot \nabla_x f_i = \frac{1}{\epsilon} Q_i + \left[\partial_t M_i + \Pi_{M_i}(\xi \cdot \nabla_x f_i) - \frac{1}{\epsilon} \Pi_{M_i} Q_i \right].$$

$\partial_t M_i + \Pi_{M_i}(\xi \cdot \nabla_x f_i) - \frac{1}{\epsilon} \Pi_{M_i} Q_i$ belongs to the space D_{M_i}. On the other hand, (17) is equivalent to $\left\langle H(\partial_t M_i + \xi \cdot \nabla_x f_i - \frac{1}{\epsilon} Q_i) \right\rangle = 0$, which implies $\partial_t M_i + \Pi_{M_i}(\xi \cdot \nabla_x f_i) - \frac{1}{\epsilon} \Pi_{M_i} Q_i$ is orthogonal to the space D_{M_i}. Consequently, $\partial_t M_i + \Pi_{M_i}(\xi \cdot \nabla_x f_i) - \frac{1}{\epsilon} \Pi_{M_i} Q_i = 0$ and f_i satisfies the Boltzmann equation. □

Corresponding to (16)-(17), the kinetic/fluid system from the multispecies BGK model (4) is:

$$\partial_t g_i + (I - \Pi_{M_i})(\xi \cdot \nabla_x g_i) = \frac{1}{\epsilon}\left[\frac{\nu_i}{\epsilon}(I - \Pi_{M_i})\widetilde{M}_i - \nu_i g_i - (I - \Pi_{M_i})(\xi \cdot \nabla_x M_i)\right], \tag{19}$$

$$\partial_t U_i + \nabla_x \cdot F(U_i) + \epsilon \nabla_x \cdot \langle m_i \xi H g_i \rangle = \frac{1}{\epsilon}\langle m_i H Q_i \rangle. \tag{20}$$

The calculation on the first term of the right side (19) gives

$$\begin{aligned}(I - \Pi_{M_i})\widetilde{M}_i &= \widetilde{M}_i - M_i\left[1 + \frac{\xi - u_i}{T_i/m_i}\cdot(\widetilde{u}_i - u_i) + \left(\frac{|\xi - u_i|^2}{2T_i/m_i} - \frac{d}{2}\right)\left(\frac{\widetilde{T}_i - T_i}{T_i} + \frac{|\widetilde{u}_i - u_i|^2}{T_i/m_i}\right)\right] \\ &= \widetilde{M}_i - \left(M_i + \partial_{u_i} M_i \cdot (\widetilde{u}_i - u_i) + \partial_{T_i} M_i(\widetilde{T}_i - T_i + m_i|\widetilde{u}_i - u_i|^2)\right).\end{aligned} \tag{21}$$

In the next two sections we will show that the kinetic/fluid system (19) - (20) recovers the fluid approximation of the Euler and CNS equations as the standard Chapman-Enskog expansion on the BGK model.

3.2 The Euler system

As $\epsilon \to 0$, $Q_i = 0 \Rightarrow \langle HQ_i \rangle = 0$. The equations in (5) - (7) imply that $u_i = u_k = u, T_i = T_k = T$. Under the common velocity and temperature,

$$f_i = \overline{M_i}(U) = n_i\left(\frac{m_i}{2\pi T}\right)^{d/2}\exp\left(-\frac{m_i|\xi - u|^2}{2T}\right), \tag{22}$$

and

$$g_i = 0.$$

Hence, the equation (20) automatically turns into the Euler equations:

$$\begin{aligned}\partial_t \rho_i + \nabla_x \cdot (\rho_i u) &= 0, \\ \partial_t \rho u + \nabla_x \cdot (\rho u \otimes u + nT\bar{\bar{I}}) &= 0, \\ \partial_t E + \nabla_x \cdot [(E + nT)u] &= 0.\end{aligned} \tag{23}$$

3.3 Chapman-Enskog expansion and the Navier-Stokes system

When $\epsilon \ll 1$, from (10), the states of species are close to the equilibrium after the collision process (see [1]):

$$u_i - u \sim O(\epsilon) \quad \text{and} \quad T_i - T \sim O(\epsilon). \tag{24}$$

Consequently, $(I - \Pi_{M_i})\widetilde{M}_i$ in (21) is the difference of $\widetilde{M}_i$ and its linear approximation at M_i with a second order residual, which means

$$(I - \Pi_{M_i})\widetilde{M}_i \sim O(\epsilon^2). \tag{25}$$

Thus, (19) gives

$$g_i = -\frac{1}{\nu_i}(I - \Pi_{M_i})(\xi \cdot \nabla_x M_i) + O(\epsilon). \tag{26}$$

Through the calculations as in [2], we have

$$(I - \Pi_{M_i})(\xi \cdot \nabla_x M_i) = \left[B : \left(\nabla_x u_i + (\nabla_x u_i)^T - \frac{2}{d}(\nabla_x \cdot u_i)\bar{\bar{I}}\right) + A \cdot \frac{\nabla_x T_i}{\sqrt{T_i}}\right] M_i + O(\epsilon),$$

where $\bar{\bar{I}}$ is the identity matrix, and

$$A = \left(\frac{|\xi - u_i|^2}{2T_i/m_i} - \frac{d+2}{2}\right)\frac{\xi - u_i}{\sqrt{T_i}}, \qquad B = \frac{1}{2}\left[\frac{(\xi - u_i)\otimes(\xi - u_i)}{2T_i/m_i} - \frac{|\xi - u_i|^2}{dT_i/m_i}\bar{\bar{I}}\right].$$

Plugging the leading term of (26) into (20),

$$\partial_t U_i + \nabla_x \cdot F(U_i) = \frac{1}{\epsilon}\langle m_i H Q_i\rangle + \epsilon \nabla_x \cdot \left\langle m_i \xi H \frac{1}{\nu_i}(I - \Pi_{M_i})(\xi \cdot \nabla_x M_i)\right\rangle + O(\epsilon^2). \tag{27}$$

Note

$$\epsilon \left\langle m_i \xi H \frac{1}{\nu_i}(I - \Pi_{M_i})(\xi \cdot \nabla_x M_i)\right\rangle = -\begin{pmatrix} 0 \\ \sigma_i \\ \sigma_i u_i + q_i \end{pmatrix},$$

which is nothing but the CNS system's viscosity and heat conduction parts for the species i. The rescaled viscosity tensor is

$$\sigma_i = -\eta_i \left(\nabla_x u_i + (\nabla_x u_i)^T - \frac{2}{d}(\nabla_x \cdot u_i)\bar{\bar{I}}\right)$$

with the viscosity coefficient $\eta_i = \epsilon T_i \frac{n_i}{\nu_i}$. The heat flux is

$$q_i = -\kappa_i \nabla_x T_i$$

with the thermal conductivity coefficient $\kappa_i = \epsilon \frac{d+2}{2} T_i \frac{n_i}{m_i \nu_i}$.

From (27), the CNS equations of species i can be written as

$$\partial_t \rho_i + \nabla_x \cdot (\rho_i u) = -\nabla_x \cdot (\rho_i u_i - \rho_i u), \tag{28a}$$

$$\partial_t \rho_i u_i + \nabla_x \cdot (\rho_i u_i \otimes u_i + n_i T_i \bar{\bar{I}} + \sigma_i) = \frac{1}{\epsilon}\langle m_i \xi Q_i\rangle + O(\epsilon^2), \tag{28b}$$

$$\partial_t E_i + \nabla_x \cdot [(E_i + n_i T_i)u_i + \sigma_i u_i + q_i] = \frac{1}{\epsilon}\left\langle \frac{m_i}{2}|\xi|^2 Q_i\right\rangle + O(\epsilon^2). \tag{28c}$$

(28a) is exactly the same with the first equation of CNS for the mixture (11)-(12). To prove that the system (28) is the approximation to (11)-(12) in $O(\epsilon^2)$, we need the following lemma.

Lemma 3. *If $u_i - u_k \sim O(\epsilon)$ and $T_i - T_k \sim O(\epsilon)$ ($\epsilon \ll 1$), then:*

$$\sum_i \rho_i u_i \otimes u_i = \rho u \otimes u + O(\epsilon^2), \tag{29}$$

$$\sum_i n_i T_i = nT + O(\epsilon^2), \tag{30}$$

$$\sum_i \frac{1}{2}\rho_i |u_i|^2 u_i = \frac{1}{2}\rho |u|^2 u + O(\epsilon^2). \tag{31}$$

Proof. We prove (29), which is equivalent to

$$\rho \sum_i \rho_i u_i \otimes u_i = \rho u \otimes \rho u + O(\epsilon^2). \tag{32}$$

Recall the definition of ρ, u and T:

$$\rho = \sum_i \rho_i, \quad \rho u = \sum_i \rho_i u_i,$$
$$n\frac{d}{2}T + \frac{\rho}{2}|u|^2 = \sum_i E_i = \sum_i n_i \frac{d}{2} T_i + \frac{\rho_i}{2}|u_i|^2, \tag{33}$$

and write the vector $u_i = \left(u_i^{(j)}\right)_{j=1,2,\ldots,d}$. When $j \neq s$, the left hand side in (32) is

$$(\mathbb{LHS})_{j,s} = \sum_k \rho_k \sum_i \rho_i u_i^{(j)} u_i^{(s)} = \sum_k \sum_i \rho_k \rho_i u_i^{(j)} u_i^{(s)},$$

while the right hand side in (32) is

$$(\mathbb{RHS})_{j,s} = \sum_k \rho_k u_k^{(s)} \sum_i \rho_i u_i^{(j)} = \sum_k \sum_i \rho_k \rho_i u_i^{(j)} u_k^{(s)}.$$

Thus,

$$(\mathbb{LHS} - \mathbb{RHS})_{j,s} = \sum_k \sum_i \rho_k \rho_i u_i^{(j)} \left(u_i^{(s)} - u_k^{(s)} \right).$$

The subscript i and k are exchangeable; then

$$(\mathbb{LHS} - \mathbb{RHS})_{j,s} = \sum_k \sum_i \rho_k \rho_i u_k^{(j)} \left(u_k^{(s)} - u_i^{(s)} \right).$$

Add up these two results, we can get

$$(\mathbb{LHS} - \mathbb{RHS})_{j,s} = \frac{1}{2} \sum_k \sum_i \rho_k \rho_i \left(u_i^{(j)} - u_k^{(j)} \right) \left(u_i^{(s)} - u_k^{(s)} \right) \sim O(\epsilon^2)$$

as in (29). The same approach with the energy conservation in (33) indicates that

$$n \frac{d}{2} T - \sum_i n_i \frac{d}{2} T_i = \sum_i \frac{\rho_i}{2} |u_i|^2 - \frac{\rho}{2} |u|^2 \sim O(\epsilon^2)$$

as in (30), which is only the case $j = s$ in (32). Multiplying the equation (31) by the total mass density ρ, the left hand side is

$$\mathbb{LHS} = \frac{\rho}{2} \sum_i \rho_i \left| u_i \right|^2 u_i = \frac{1}{2} \sum_j \sum_i \rho_j \rho_i \left| u_i \right|^2 u_i,$$

while the right hand side

$$\mathbb{RHS} = \frac{\rho}{2} \rho \left| u \right|^2 u = \frac{1}{2} \rho \sum_i \rho_i \left| u_i \right|^2 u + \dot{O(\epsilon^2)} = \frac{1}{2} \sum_j \sum_i \rho_j \rho_i \left| u_i \right|^2 u_j + \dot{O(\epsilon^2)}.$$

We have

$$\mathbb{LHS} - \mathbb{RHS} = \frac{1}{2} \sum_j \sum_i \rho_j \rho_i \left| u_i \right|^2 (u_i - u_j).$$

Exchange the subscript i and j and we finally prove the result

$$\mathbb{LHS} - \mathbb{RHS} = \frac{1}{2} \sum_j \sum_i \rho_j \rho_i \left| u_i \right|^2 (u_i - u_j) \sim O(\epsilon^2)$$

as in (31). □

Recalling the conservation laws (2) and summing up the second moments (28b) for all species, we obtain the momentum equations of the compressible Navier-Stokes system for the mixture:

$$\partial_t (\rho u) + \nabla_x \cdot (\rho u \otimes u + P) = 0, \tag{34}$$

$$P = nT \bar{\bar{I}} - \eta \left(\nabla_x u + (\nabla_x u)^T - \frac{2}{d} (\nabla_x \cdot u) \bar{\bar{I}} \right) + O(\epsilon^2).$$

The viscosity coefficient: $\eta = \epsilon T \sum_i \frac{n_i}{\nu_i}$.

Summing up the energy equation (28c) for all species and using (31) lead to

$$\begin{aligned}\sum_i (E_i + n_i T_i)u_i &= \sum_i \left(\frac{1}{2}\rho_i |u_i|^2 u_i + \frac{d+2}{2} n_i T_i u_i\right) \\ &= \frac{1}{2}\rho |u|^2 u + \frac{d+2}{2} nTu + \sum_i \frac{d+2}{2} n_i T_i (u_i - u) + O(\epsilon^2) \\ &= \frac{1}{2}\rho |u|^2 u + \frac{d+2}{2} nTu + \frac{d+2}{2} T \sum_i n_i (u_i - u) + O(\epsilon^2)\end{aligned}$$

(note that the third term is $O(\epsilon)$). Therefore, we obtain the third equation of CNS :

$$\partial_t E + \nabla_x \cdot [(Eu + P)u + q] = 0, \tag{35}$$

$$q = \frac{d+2}{2} T \sum_i n_i (u_i - u) - \kappa \nabla_x T + O(\epsilon^2),$$

$\kappa = \epsilon \frac{d+2}{2} T \sum_i \frac{n_i}{m_i \nu_i}$ is the thermal conductivity coefficient.

Thus, the system (28a)-(28c) is a second order in ϵ approximation of the CNS system arising from the Chapman-Enskog expansion of the BGK system (11)-(12) derived in [1].

4 Asymptotic-preserving numerical approximations

In this section, we will present an asymptotic-preserving numerical approximation of the coupling system (19)-(20). Given the fixed time step and space mesh size, we will show that our numerical scheme approximates the discretization of the Euler system with error $O(\epsilon)$, thus asymptotically preserves the Euler limit. It is also consistent with the CNS system if $\Delta x, \Delta t \ll \epsilon$.

This scheme is an extension of the scheme [3] for single species, and it recovers the method of [3] if there is only one species.

4.1 Time discretization

In the first step, we give the AP time discretization. Space and velocity discretizations will be studied in the next subsection. We denote a fixed time step Δt and a sequence of discrete time $t_l = l\Delta t$, $l \in \mathbb{N}$. Thus, $g_i^l(x, \xi) = g_i(t_l, x, \xi)$, $U_i^l(x) = U_i(t_l, x)$.

In the kinetic equation (19), the term $\frac{\nu_i}{\epsilon^2}(I - \Pi_{M_i})\widetilde{M_i}$ is $O(1)$ from (25), thus is not a stiff term; so it will be treated explicitly. For the stability independent of ϵ, we treat g_i term in the collision part implicitly. This semi-implicit scheme on the kinetic equation has the expression

$$\frac{g_i^{l+1} - g_i^l}{\Delta t} + (I - \Pi_{M_i^l})(\xi \cdot \nabla_x g_i^l) = \frac{1}{\epsilon}\left[\frac{\nu_i^l}{\epsilon}(I - \Pi_{M_i^l})\widetilde{M_i}^l - \nu_i^l g_i^{l+1} - (I - \Pi_{M_i^l})(\xi \cdot \nabla_x M_i^l)\right]. \tag{36}$$

Now, we discretize the second equation (20). In (20), there are three scales: $O(\frac{1}{\epsilon})$ collision term; $O(1)$ convection term and $O(\epsilon)$ diffusion term. The latest two terms essentially come from the molecule convection. We will use splitting method to separately calculate the collision and convection terms in (20)

$$\frac{U_i^{l+\frac{1}{2}} - U_i^l}{\Delta t} + \nabla_x \cdot F(U_i^l) + \epsilon \nabla_x \cdot \left\langle m_i \xi H g_i^l \right\rangle = 0, \tag{37}$$

$$\frac{U_i^{l+1} - U_i^{l+\frac{1}{2}}}{\Delta t} = \frac{1}{\epsilon}\left\langle m_i H Q_i^{l+1} \right\rangle. \tag{38}$$

We order these steps in the following way:

$$\frac{U_i^{l+\frac{1}{2}}-U_i^l}{\Delta t}=\frac{1}{\epsilon}\left\langle m_i H Q_i^{l+\frac{1}{2}}\right\rangle, \tag{39}$$

$$\begin{aligned}&\frac{g_i^{l+1}-g_i^l}{\Delta t}+\left(I-\Pi_{M_i^{l+\frac{1}{2}}}\right)\left(\xi\cdot\nabla_x g_i^l\right)\\&=\frac{1}{\epsilon}\left[\frac{\nu_i^{l+\frac{1}{2}}}{\epsilon}\left(I-\Pi_{M_i^{l+\frac{1}{2}}}\right)\widetilde{M_i}^{l+\frac{1}{2}}-\nu_i^{l+\frac{1}{2}}g_i^{l+1}-\left(I-\Pi_{M_i^{l+\frac{1}{2}}}\right)\left(\xi\cdot\nabla_x M_i^{l+\frac{1}{2}}\right)\right],\end{aligned} \tag{40}$$

$$\frac{U_i^{l+1}-U_i^{l+\frac{1}{2}}}{\Delta t}+\nabla_x\cdot F(U_i^{l+\frac{1}{2}})+\epsilon\nabla_x\cdot\left\langle m_i\xi H g_i^{l+1}\right\rangle=0. \tag{41}$$

Although (39) is fully implicit, note the results in (5)-(7), one can write it as

$$\begin{aligned}\frac{\rho_i^{l+\frac{1}{2}}-\rho_i^l}{\Delta t}&=0,\\\frac{\rho_i^{l+\frac{1}{2}}u_i^{l+\frac{1}{2}}-\rho_i^l u_i^l}{\Delta t}&=\frac{1}{\epsilon}\sum_k 2\mu_{ik}\chi_{ik}n_i^{l+\frac{1}{2}}n_k^{l+\frac{1}{2}}\left[u_k^{l+\frac{1}{2}}-u_i^{l+\frac{1}{2}}\right],\\\frac{E_i^{l+\frac{1}{2}}-E_i^l}{\Delta t}&=\frac{1}{\epsilon}\sum_k 2\mu_{ik}\chi_{ik}n_i^{l+\frac{1}{2}}n_k^{l+\frac{1}{2}}\left[\left(u_k^{l+\frac{1}{2}}-u_i^{l+\frac{1}{2}}\right)u_i^{l+\frac{1}{2}}\right.\\&\quad\left.+\frac{2}{m_i+m_k}\left(e_k^{l+\frac{1}{2}}-e_i^{l+\frac{1}{2}}+m_k\left|u_k^{l+\frac{1}{2}}-u_i^{l+\frac{1}{2}}\right|^2/2\right)\right].\end{aligned} \tag{39$'$}$$

This implicit scheme satisfies the conservation laws as well as the limit properties (see Remark 5). Simplify the above and we will obtain a linear system

$$n_i^{l+\frac{1}{2}}=n_i^l, \tag{42}$$

$$u_i^{l+\frac{1}{2}}-u_i^l=\frac{\Delta t}{\epsilon}\sum_k 2\chi_{ik}\frac{m_k n_k^{l+\frac{1}{2}}}{m_k+m_i}\left[u_k^{l+\frac{1}{2}}-u_i^{l+\frac{1}{2}}\right], \tag{43}$$

$$E_i^{l+\frac{1}{2}}-E_i^l=\frac{\Delta t}{\epsilon}\sum_k\frac{4m_i m_k}{(m_i+m_k)^2}\chi_{ik}n_i^{l+\frac{1}{2}}n_k^{l+\frac{1}{2}}\left[\frac{1}{2}(m_i-m_k)u_k^{l+\frac{1}{2}}u_i^{l+\frac{1}{2}}+\frac{E_k^{l+\frac{1}{2}}}{n_k^{l+\frac{1}{2}}}-\frac{E_i^{l+\frac{1}{2}}}{n_i^{l+\frac{1}{2}}}\right]. \tag{44}$$

Suppose that there are K species in the mixture, let $\overrightarrow{u}=(u_1\ u_2\ ...\ u_K)$. Due to (42), (43) is a linear system for $\overrightarrow{u}$. Once $\overrightarrow{u}^{l+\frac{1}{2}}$ is obtained, (44) is a linear system for $\overrightarrow{E}=(E_1\ E_2\ ...\ E_K)$. Thus, although the right hand side of (39) is nonlinear, we only need to solve linear systems. (40) is clearly linear for g_i^{l+1} which can be obtained easily.

Proposition 4. *(i) The time discretizations as (39) - (41) give a scheme consistent with the Euler system (23) when $\epsilon\to 0$;*

(ii) for small ϵ, the scheme (39) - (41) is asymptotically the $O(\epsilon^2)$ approximation to an explicit time discretization of CNS system (11) - (12).

Proof. (i) When $\epsilon\to 0$, the implicit collision scheme (39) leads to $u_i^{l+\frac{1}{2}}=u^{l+\frac{1}{2}}$ and $T_i^{l+\frac{1}{2}}=T^{l+\frac{1}{2}}$ for $\forall i$, and (41) becomes the following forward Euler discretization in time of the Euler system:

$$\text{(Euler):}\qquad\frac{U^{l+1}-U^{l+\frac{1}{2}}}{\Delta t}+\nabla_x\cdot F(U^{l+\frac{1}{2}})=0. \tag{45}$$

(ii) From (21), the first term in the right hand side of (40) is $O(1)$. The semi-implicit scheme in equation (40) yields

$$g_i^{l+1}=-\frac{1}{\nu_i^{l+1/2}}\left(I-\Pi_{M_i^{l+\frac{1}{2}}}\right)\left(\xi\cdot\nabla_x M_i^{l+\frac{1}{2}}\right)+O(\epsilon).$$

Applying it into (41), we get

$$\frac{U_i^{l+1}-U_i^{l+\frac{1}{2}}}{\Delta t}+\nabla_x\cdot F(U_i^{l+\frac{1}{2}})=\epsilon\nabla_x\cdot\left\langle m_i\xi H\frac{1}{\nu_i^{l+1/2}}\left(I-\Pi_{M_i^{l+\frac{1}{2}}}\right)\left(\xi\cdot\nabla_x M_i^{l+\frac{1}{2}}\right)\right\rangle+O(\epsilon^2), \tag{46}$$

which is an $O(\epsilon^2)$ approximation to the forward Euler discretization in time of CNS for species i (27). The summation over all species is also consistent with multispecies CNS as $u_i-u\sim O(\epsilon)$ and $T_i-T\sim O(\epsilon)$, which has been proved in Section 3.3. □

Remark 5. *In this paper, we derive the implicit scheme (42)-(44) for the collision process of the consistent BGK model (4). Although the collision term is a nonlinear function of the macroscopic quantities, the Maxwell particle relations (5)-(7) provide a method to solve a linear system. It is easy to check that the scheme has the conservation property during the collision (39′), namely* $\rho_i^{l+\frac{1}{2}}=\rho_i^l$, $\sum_i\rho_i^{l+\frac{1}{2}}u_i^{l+\frac{1}{2}}=\sum_i\rho_i^l u_i^l$ *and* $\sum_i E_i^{l+\frac{1}{2}}=\sum_i E_i^l$. *It also satisfies that at the limit* $(\epsilon=0)$ $u_i^{l+\frac{1}{2}}=u_k^{l+\frac{1}{2}}$ *and* $T_i^{l+\frac{1}{2}}=T_k^{l+\frac{1}{2}}$ *for* $\forall i,k$.

4.2 Space discretization

The terms that need the spatial discretizations include: the fluxes on the left-hand side of both (40) and (41); and the diffusion term in (41). The convection terms will be discretized by upwind scheme. For the diffusion term, the central differences defined on two staggered grids is used. Since in (41) g_i's influence on U_i is $O(\epsilon)$ as diffusion, the explicit central discretization for the leading term of $(I-\Pi_{M_i})(\xi\cdot\nabla_x M_i)$ in (41) will be taken. The critical steps are shown in the remainder of this section.

We use a uniform grid $x_{m+\frac{1}{2}}$ and define x_m the center of the cell $\left[x_{m-\frac{1}{2}},x_{m+\frac{1}{2}}\right]$. The mesh size $\Delta x=x_{m+\frac{1}{2}}-x_{m-\frac{1}{2}}=x_{m+1}-x_m$, $m\in\mathbb{N}$. The macroscopic U_i^l of species i are discretized at the grid center points as $U_{i,m}^l=U_i(t_l,x_m)$ while the microscopic g_i^l are at the grid end points as $g_{i,m+\frac{1}{2}}^l=g_i(t_l,x_{m+\frac{1}{2}},\xi)$. The velocity is discretized evenly in a bounded domain. The rectangular quadratures are applied to approximate the integrals with respect to the velocity. For a simplified expression, we will not explicitly express the discrete velocity for the microscopic functions. The numerical scheme for the system (39) - (41) is

$$\frac{U_{i,m}^{l+\frac{1}{2}}-U_{i,m}^l}{\Delta t}=\frac{1}{\epsilon}\langle m_i H Q_{i,m}^{l+\frac{1}{2}}\rangle, \tag{47}$$

$$\text{(MM):}\quad \frac{g_{i,m+\frac{1}{2}}^{l+1}-g_{i,m+\frac{1}{2}}^l}{\Delta t}+\left(I-\Pi_{M_{i,m+1/2}^{l+1/2}}\right)\left(\xi\cdot\partial_x g_{i,m+\frac{1}{2}}^l\right) \tag{48}$$

$$=\frac{1}{\epsilon}\left[\frac{\nu_{i,m+\frac{1}{2}}^{l+\frac{1}{2}}}{\epsilon}(I-\Pi_{M_{i,m+1/2}^{l+1/2}})\widetilde{M}_{i,m+\frac{1}{2}}^{l+\frac{1}{2}}-\nu_{i,m+\frac{1}{2}}^{l+\frac{1}{2}}g_{i,m+\frac{1}{2}}^{l+1}-(I-\Pi_{M_{i,m+1/2}^{l+1/2}})\left(\xi\frac{M_{i,m+1}^{l+\frac{1}{2}}-M_{i,m}^{l+\frac{1}{2}}}{\Delta x}\right)\right],$$

$$\frac{U_{i,m}^{l+1}-U_{i,m}^{l+\frac{1}{2}}}{\Delta t}+\frac{F_{m+\frac{1}{2}}(U_i^{l+\frac{1}{2}})-F_{m-\frac{1}{2}}(U_i^{l+\frac{1}{2}})}{\Delta x}+\epsilon\left\langle m_i\xi H\frac{g_{i,m+\frac{1}{2}}^{l+1}-g_{i,m-\frac{1}{2}}^{l+1}}{\Delta x}\right\rangle=0. \tag{49}$$

The flux term in (48) is approximated by a first order upwind scheme

$$\xi\cdot\partial_x g_{i,m+\frac{1}{2}}^l\approx\frac{\Phi_{m+\frac{1}{2}}(g_i^l)-\Phi_{m-\frac{1}{2}}(g_i^l)}{\Delta x},$$

where

$$\Phi_{m+\frac{1}{2}}(g_i^l)=\xi^+g_{i,m+\frac{1}{2}}^l+\xi^-g_{i,m+\frac{3}{2}}^l$$

(we define $\xi^\pm=\frac{\xi\pm|\xi|}{2}$). The projection operator $\Pi_{M_{i,m+1/2}}$ is chosen by $\Pi_{M_{i,m+1/2}}\approx\frac{\Pi_{M_{i,m}}+\Pi_{M_{i,m+1}}}{2}$. The fluid flux $F_{m+\frac{1}{2}}$ in (49) is discretized by the kinetic flux vector splitting scheme in [22]:

$$F_{m+\frac{1}{2}}(U_i^{l+\frac{1}{2}})=\left\langle m_i H\left(\xi^+M_{i,m}^l+\xi^-M_{i,m+1}^l\right)\right\rangle. \tag{50}$$

The asymptotic behavior of scheme when $\epsilon \ll 1$ can be understood as following. For $\epsilon \ll 1$, the leading order in (48) gives

$$g_{i,m+\frac{1}{2}}^{l+1} \approx -\frac{1}{\nu_{i,m+1/2}^{l+1/2}} \left(I - \Pi_{M_{i,m+1/2}^{l+1/2}}\right) \left(\xi \frac{M_{i,m+1}^{l+\frac{1}{2}} - M_{i,m}^{l+\frac{1}{2}}}{\Delta x}\right).$$

Plugging it into (49) gives

$$\begin{aligned} \text{(NS/MM):} \quad & \frac{U_{i,m}^{l+1} - U_{i,m}^{l+\frac{1}{2}}}{\Delta t} + \frac{F_{m+\frac{1}{2}}(U_i^{l+\frac{1}{2}}) - F_{m-\frac{1}{2}}(U_i^{l+\frac{1}{2}})}{\Delta x} \qquad (51) \\ = & \frac{\epsilon}{\Delta x} \left\langle m_i \xi H \left[\frac{1}{\nu_{i,m+\frac{1}{2}}^{l+1/2}} (I - \Pi_{M_{i,m+1/2}^{l+1/2}}) (\xi \frac{M_{i,m+1}^{l+\frac{1}{2}} - M_{i,m}^{l+\frac{1}{2}}}{\Delta x}) - \frac{1}{\nu_{i,m-\frac{1}{2}}^{l+1/2}} (I - \Pi_{M_{i,m-1/2}^{l+1/2}}) (\xi \frac{M_{i,m}^{l+\frac{1}{2}} - M_{i,m-1}^{l+\frac{1}{2}}}{\Delta x}) \right] \right\rangle, \end{aligned}$$

which is a second order approximation of the CNS equation (27). Thus the scheme is asymptotic preserving (AP) for the Euler limit ($\Delta x, \Delta t = O(1)$, $\epsilon \ll 1$). (51) is also consistent to the CNS if $\Delta x, \Delta t \ll O(\epsilon)$.

To reduce numerical viscosity, we will use the second order upwind scheme (in the sense of Van Leer in [25]) to reduce the numerical viscosity. Such a scheme needs to use the slope limiter. In our numerical tests, the classical minmod slope limiter (see [20]) is applied.

For numerical comparisons, we also present the schemes for the BGK model and the CNS equations in the following two subsections.

4.3 A numerical approximation of the BGK model

To discretize the 1-D BGK model:

$$\partial_t f_i + \xi \partial_x f_i = \frac{\nu_i}{\epsilon} \left(\widetilde{M}_i - f_i\right),$$

we use the splitting method: solve the collision process by implicit scheme and the convection process by first order explicit upwind scheme:

$$(S_i): \qquad \frac{f_{i,m}^{l+\frac{1}{2}} - f_{i,m}^{l}}{\Delta t} = \frac{\nu_{i,m}^{l+\frac{1}{2}}}{\epsilon} \left(\widetilde{M}_{i,m}^{l+\frac{1}{2}} - f_{i,m}^{l+\frac{1}{2}}\right) \equiv \frac{1}{\epsilon} Q_{i,m}^{l+\frac{1}{2}}, \qquad (52)$$

$$\frac{f_{i,m}^{l+1} - f_{i,m}^{l+\frac{1}{2}}}{\Delta t} + \frac{\Phi_{m+\frac{1}{2}}(f_i^{l+\frac{1}{2}}) - \Phi_{m-\frac{1}{2}}(f_i^{l+\frac{1}{2}})}{\Delta x} = 0. \qquad (53)$$

Here $f_{i,m}^l = f_i(t_l, x_m)$ and $\Phi_{m+\frac{1}{2}}(f_i^{l+\frac{1}{2}}) = \xi^+ f_{i,m}^{l+\frac{1}{2}} + \xi^- f_{i,m+1}^{l+\frac{1}{2}}$. The conservation of mass leads to $\nu_{i,m}^{l+\frac{1}{2}} = \nu_{i,m}^l$; $\widetilde{M}_{i,m}^{l+\frac{1}{2}}$ is a nonlinear function of the moments of $f_{i,m}^{l+\frac{1}{2}}$, which is $U_{i,m}^{l+\frac{1}{2}}$. We take the moments of (52):

$$\frac{U_{i,m}^{l+\frac{1}{2}} - U_{i,m}^{l}}{\Delta t} = \frac{1}{\epsilon} \left\langle m_i H Q_{i,m}^{l+\frac{1}{2}} \right\rangle.$$

The same process (42)-(44) will solve $U_{i,m}^{l+\frac{1}{2}}$ by inverting linear systems. Consequently, we get $\widetilde{M}_{i,m}^{l+\frac{1}{2}}$, and solve (52) for $f_{i,m}^{l+\frac{1}{2}}$.

4.4 A numerical approximation of the CNS equations

In the 1-D CNS, the pressure $P = nT$ and the equations (11) are:

$$\begin{aligned} \partial_t \rho_i + \partial_x(\rho_i u) &= -\partial_x J_i, \\ \partial_t(\rho u) + \partial_x(\rho u^2 + nT) &= 0, \qquad (54) \\ \partial_t E + \partial_x\left[(E + nT)u\right] &= \partial_x \left(\kappa \partial_x T - \frac{3}{2} T \sum_i \frac{J_i}{m_i}\right). \end{aligned}$$

Here the thermal conductivity coefficients $\kappa = \epsilon \frac{3}{2} T \sum_i \frac{n_i}{m_i \nu_i}$, and the diffusion velocity $J_i = -\epsilon \sum_k L_{ik} \frac{\partial_x (n_k T)}{\rho_k}$, of which L_{ik} is defined in [1] as a function of densities. The left hand side are the same as the Euler equations, and we will replace them by $\partial_t U + \partial_x F(U)$ and implement the kinetic flux vector splitting scheme (50) on the flux terms. The right hand side is the diffusion terms which are discretized by the central discretization

$$\text{(NS)} \quad \frac{U_m^{l+1} - U_m^l}{\Delta t} + \frac{F^l_{m+\frac{1}{2}}(U^l) - F^l_{m-\frac{1}{2}}(U^l)}{\Delta x} \tag{55}$$
$$= \frac{1}{\Delta x} \begin{pmatrix} -\left(J^l_{i,m+\frac{1}{2}} - J^l_{i,m-\frac{1}{2}}\right) \\ 0 \\ \left(\kappa^l_{m+\frac{1}{2}} \frac{T^l_{m+1} - T^l_m}{\Delta x} - \frac{3}{2} T^l_{m+\frac{1}{2}} \sum_i \frac{J^l_{i,m+\frac{1}{2}}}{m_i}\right) - \left(\kappa^l_{m-\frac{1}{2}} \frac{T^l_m - T^l_{m-1}}{\Delta x} - \frac{3}{2} T^l_{m-\frac{1}{2}} \sum_i \frac{J^l_{i,m-\frac{1}{2}}}{m_i}\right) \end{pmatrix},$$

where

$$J^l_{i,m+\frac{1}{2}} = -\epsilon \sum_k \frac{L^l_{ik,m+\frac{1}{2}}}{\rho^l_{k,m+\frac{1}{2}}} \left(\frac{n^l_{k,m+1} T^l_{m+1} - n^l_{k,m} T^l_m}{\Delta x}\right).$$

The quantities at the half grid $T_{m+\frac{1}{2}}$, $\kappa_{m+\frac{1}{2}}$, $\rho_{k,m+\frac{1}{2}}$and $L_{ik,m+\frac{1}{2}}$ will be estimated by the average of the nearby two grids as $T_{m+\frac{1}{2}} \approx \frac{T_{m+1} + T_m}{2}$.

5 Numerical results

Without loss of generality, all numerical examples studied in this paper will be conducted for a two-species mixture. We first show the numerical results for the one-dimensional BGK model (4), to investigate the behavior of the mixture. We then present several numerical solutions of the one-dimensional coupling system using (47)-(49) corresponding to the solution of the BGK model (52)-(53). To illustrate the asymptotic preserving properties, we will check that our scheme of (47)-(49) is AP to the Euler system (45) to $O(\epsilon)$, as well as captures the CNS asymptotics (55) with suitable mesh size and time step.

For convenience, we will denote our numerical schemes as following: micro/macro decomposition scheme (47)-(49) as (MM); the implicit scheme (52)-(53) for BGK model as (S_i); the numerical scheme (55) for CNS as (NS); the kinetic scheme for Euler equations (45) as (Euler); and the approximation of (MM) to CNS (51) as (NS/MM).

5.1 A space homogeneous problem

We first use the implicit scheme (S_i) for the BGK model in the space homogeneous case, to check our scheme and the behavior of the mixture in the collision process. The initial condition is

$$\begin{cases} m_a = 1, , n_a = 1, u_a = 0.5, T_a = 1 \\ m_b = 1.5, n_b = 1.2, u_b = 0.1, T_b = 0.1. \end{cases}$$

There are 200 velocity grid points in the range $[-10, 10]$ and the time step $\Delta t = 5 \times 10^{-4}$. In Fig 1, the velocities and temperatures of species a and b converge along with the different Knudsen number $\epsilon = 0.05$ and 0.01. It shows that the smaller the Knudsen number ϵ is, the faster velocities and temperatures converge into the equilibrium.

5.2 A stationary shock problem

In this example, we test the coupling system for a stationary shock. We give the initial macroscopic data on the left-hand side, while the right-hand side data are given by the Rankine-Hugoniot relations:

$$\begin{cases} m_a = 1, m_b = 1.5, n_a = n_b = 1, u_a = u_b = 1.5, T_a = T_b = 0.4, & \text{for } x \le 0; \\ m_a = 1, m_b = 1.5, n_a = n_b = 1.4019, u_a = u_b = 1.07, T_a = T_b = 0.8605, & \text{for } x > 0. \end{cases}$$

The computational domain in space is $[-0.5, 0.7]$ discretized by a uniform grids $\Delta x = 0.005$. We use a velocity grid of 200 points in domain $[-10, 10]$. To satisfy the CFL condition, the time step is taken as $\Delta t = \frac{\Delta x}{10}$.

Firstly, in Fig 2 the results by our scheme (MM) show that the density distribution function converges to the Maxwellian with diminishing Knudsen number ϵ. The results match well with the BGK model (S_i) for the stationary shock, shown in Fig 3. We illustrate the asymptotic behavior of scheme for different values of ϵ ($\epsilon = 10^{-\theta}, \theta \in \mathbb{N}$), and plot the density, velocity and temperature of the mixture as the functions of x in Fig 4, comparing them with the exact solution of the stationary shock. There exits the oscillation in the stationary shock when $\epsilon \to 0$, which results from the numerical viscosities of the finite difference method (see [14]).

Then we compare the relative numerical difference in l^1 norm with the Euler limit and investigate the convergence speed. Both micro/macro decomposition scheme (MM) and implicit BGK scheme (S_i) converge to the Euler limit in $O(\epsilon)$. We observe that the slope in Fig 5 is about 1 as expected, except when ϵ is $O(1)$, where the Euler equations are not accurate approximations to the Boltzmann equation.

5.3 Sod problem

We use the classical Sod problem [23] with the initial condition:

$$\begin{cases} n_a = 1, n_b = 1.2, u_a = u_b = 0, T_a = T_b = 1, \text{ for } x \leq 0; \\ n_a = 0.125, n_b = 0.2, u_a = u_b = 0, T_a = T_b = 0.1, \text{ for } x > 0. \end{cases}$$

We compare our micro/macro decomposition scheme (MM) with the implicit scheme on BGK (S_i) and the Euler system (Euler). The computational domain in space is $[-0.5, 0.5]$ discretized by the uniform grids $\Delta x = 0.005$. We use a velocity grid of 200 points in domain $[-10, 10]$. To satisfy the CFL condition, the time step is taken as $\Delta t = \frac{\Delta x}{10}$. Fig 6 shows that (MM) and (S_i) are almost the same for the different regimes: $\epsilon = 1$ (kinetic regime); $\epsilon = 0.01$ (transition regime) and $\epsilon = 1.0 \times 10^{-5}$ (fluid regime). Fig 7 illustrates the asymptotic behavior of (MM) for the density, velocity and the temperature of the mixture under the different Knudsen number ϵ, with its limit (Euler). We also compare the CNS system (NS) with our schemes (MM) and its asymptotics (NS/MM) in Fig 8, which indicates that (NS), NS/MM and (MM) all match well even for small ϵ.

6 Conclusion

In this work, we extend the micro-macro decomposition based asymptotic-preserving scheme, developed in [3] for single species Boltzmann equation, to multispecies Boltzmann equation. In addition to the essential properties of the scheme [3], we overcome the additional stiff source terms due to the nonconservative momentum and total energy for each species. The discretization is asymptotic-preserving in the Euler limit, and is also consistent to the Navier-Stokes limit with suitably small time step and mesh size. Moreover, the nonlinear source terms can be solved by only using linear system solvers. Numerical experiments demonstrate the efficiency and correct asymptotic behavior of this scheme.

References

[1] P. Andries, K. Aoki and B. Perthame, A consistent BGK-type model for gas mixtures, J. Stat. Phys. 106 (2002) 993-1018.

[2] C. Bardos, F. Golse and D. Levermore, Fluid dynamic limits of kinetic equations. I. Formal derivations, J. Stat. Phys. 63 (1-2) (1991) 323-344

[3] M. Bennoune, M. Lemou, and L. Mieussens, Uniformly stable numerical schemes for the Bolztmann equation preserving compressible Navier-Stokes asympotics, J. Comput. Phys. 227 (2008) 3781-3803.

[4] J.-F. Bourgat, P. Le Tallec, B. Perthame, and Y. Qiu, Coupling Boltzmann and Euler equations without overlapping, in domain decomposition methods in science and engineering (Como, 1992), 377–398, Contemp. Math. **157**, Amer. Math. Soc., Providence, RI, 1994.

[5] R. Caflisch, S. Jin and G. Russo, Uniformly accurate schemes for hyperbolic systems with relaxations, SIAM J. Num. Anal. 34 (1997) 246-281

[6] P. Degond and S. Jin, A smooth transition model between kinetic and diffusion equations, SIAM J. Numer. Anal. 42 (6) (2005) 2671-2687

[7] P. Degond, S. Jin and L. Mieussens, A smooth transition model between kinetic and hydrodynamic equations, J. Comp. Phys. 209 (2005) 665-694

[8] P. Degond, J.-G. Liu and L. Mieussens, Macroscopic fluid modes with localized kinetic upscaling effects Multiscale Model. Simul. 5 (2006) 695-1043

[9] J. H. Ferziger and H. G. Kaper, Mathematical theory of transport processes in gases, North-Holland Publishing Company (1972)

[10] F. Golse, S. Jin and C.D. Levermore, The convergence of numerical transfer schemes in diffusive regimes I: the discrete-ordinate method, SIAM J. Num. Anal. 36 (1999) 1333-1369

[11] L. Gosse and G. Toscani, An asymptotic-preserving well-balanced scheme for the hyperbolic heat equations, C.R. Math. Acad. Sci. Paris 334 (2002) 337-342

[12] M. Günther, P. Le Tallec, J.-P. Perlat, and J. Struckmeier, Numerical modeling of gas flows in the transition between rarefied and continuum regimes. Numerical flow simulation I, (Marseille, 1997), 222–241, Notes Numer. Fluid Mech., 66, Vieweg, Braunschweig, 1998.

[13] S. Jin, Efficient Asymptotic-Preserving (AP) schemes for some multiscale kinetic equations, SIAM J. Sci. Comp. 21 (1999) 441-454

[14] S. Jin and J.G. Liu, The effects of numerical viscosities I: slowly moving shocks, J. Comput. Phys. 126 (1996) 373-389

[15] S. Jin, L. Pareschi and G. Toscani, Diffusive relaxation schemes for discrete-velocity kinetic equations, SIAM J. Num. Anal. 35 (1998) 2405-2439

[16] S. Jin, L. Pareschi and G. Toscani, Uniformly accurate diffusive relaxation schemes for multiscale transport equations, SIAM J. Num. Anal. 38 (2000) 913-936

[17] A. Klar, An asymptotic-induced scheme for nonstationary transport equations in the diffusive limit, SIAM J. Num. Anal. 35 (1998) 1073-1094

[18] A. Klar, H. Neunzert, and J. Struckmeier, Transition from kinetic theory to macroscopic fluid equations: a problem for domain decomposition and a source for new algorithm, Transp. Theory and Stat. Phys. 29 (2000) 93-106

[19] M. Lemou and L. Mieussens, A new asymptotic preserving scheme based on micro-macro formulation for linear kinetic equations in the diffusion limit. SIAM J. Sci. Comput. 31 (2008) no. 1, 334-368.

[20] R. J. Leveque, Finite volume methods for hyperbolic problems, Cambridge University Press (2002)

[21] T.P. Liu and S.H. Yu, Boltzmann equation: micro-macro decompositions and positivity of shock profiles. Comm. Math. Phys. 246 (2004) no. 1, 133-179.

[22] J. C. Mandal and S. M. Deshpande, Kinetic flux vector splitting for Euler equations, Comput. & fluids 23 (2) (1994) 447-478

[23] G. A. Sod, A survey of several finite difference methods for systems of nonlinear hyperbolic conservation laws, J. Comput. Phys. 27 (1978) 1-31

[24] P. Le Tallec, and F. Mallinger, Coupling Boltzmann and Navier-Stokes equations by half fluxes, J. Comput. Phys. 136 (1997) 51-67

[25] B. van Leer, Towards the ultimate conservative difference scheme V. A second order sequel to Godunov's method, J. Comput. Phys. 32 (1979) 101-136

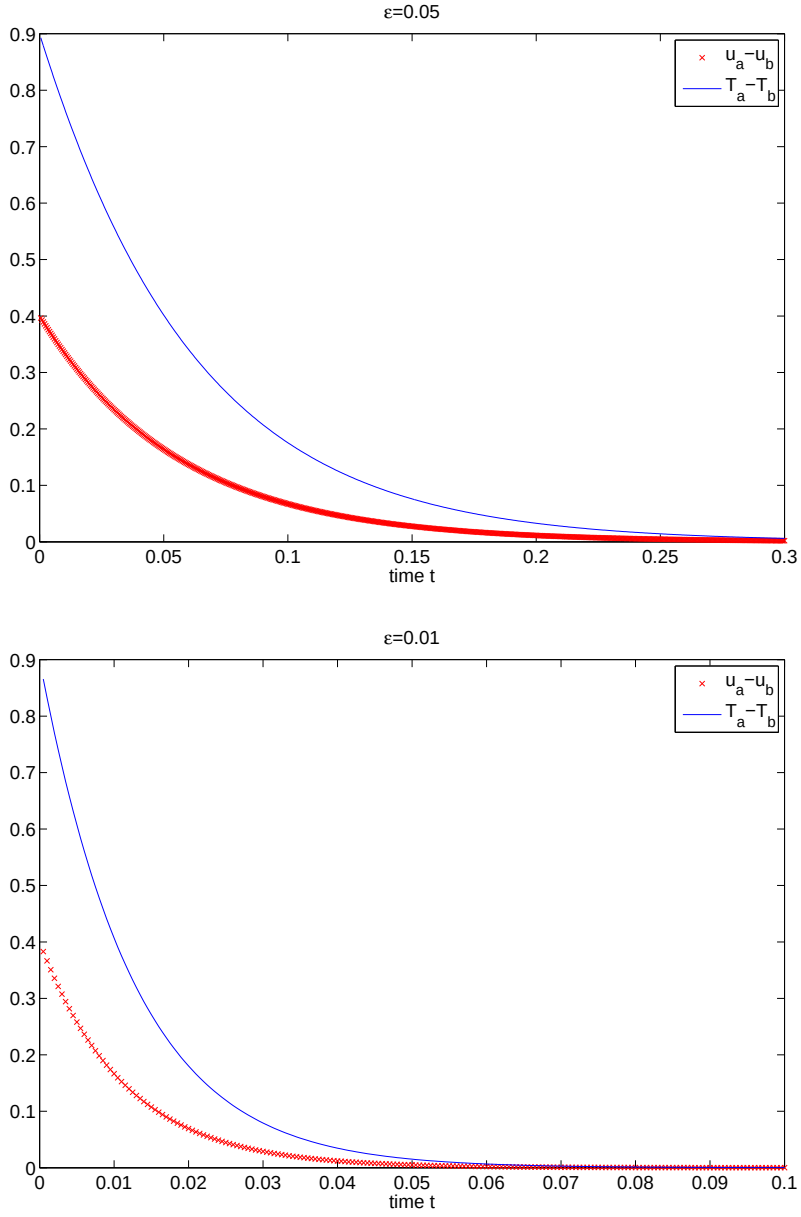

Figure 1: Space homogeneous solution by (S_i): the convergence of the velocities and temperatures between species a and b, with different Knudsen numbers $\epsilon = 0.05$ on the top, and $\epsilon = 0.01$ on the bottom.

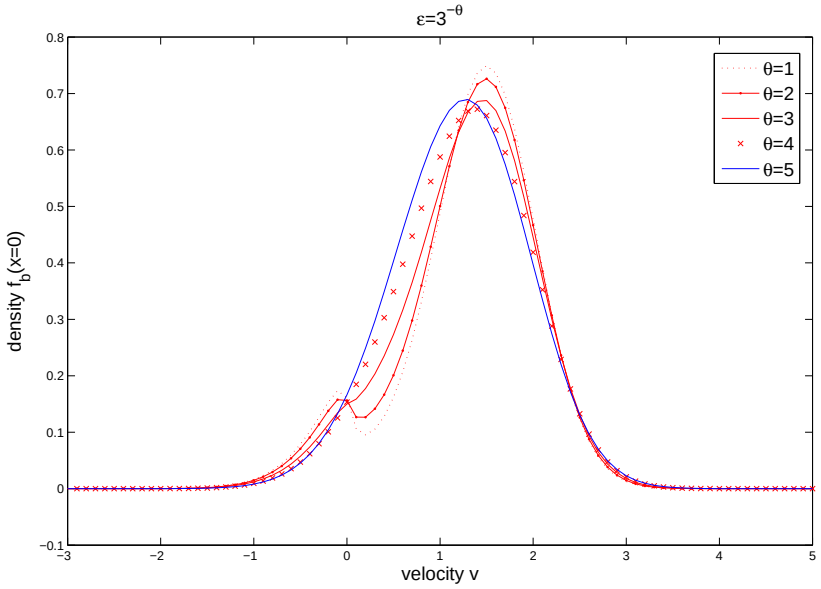

Figure 2: Stationary shock: density distribution function f_b as a function of velocity v at point $x = 0$, given by the scheme (MM) with different Knudsen numbers $\epsilon = 3^{-\theta}$, at $t = 0.1$.

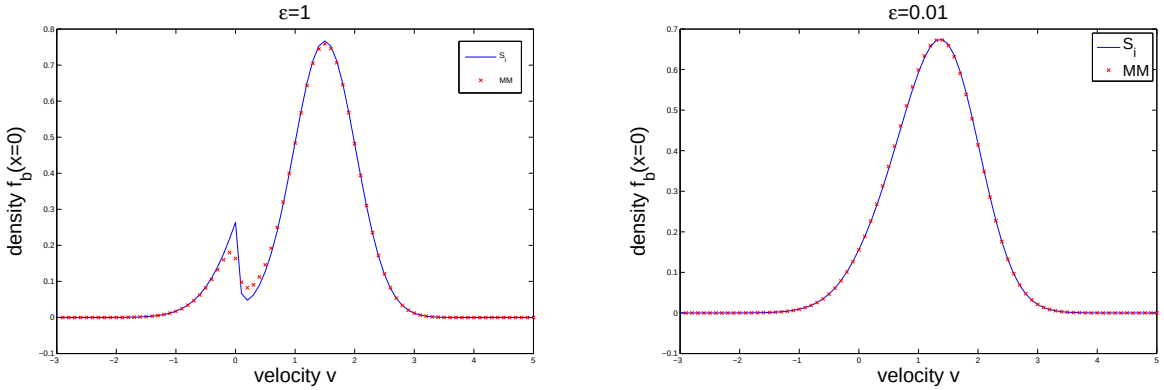

Figure 3: Stationary shock: density distribution function f_b as a function of velocity v at point $x = 0$, given by the scheme (MM) with different Knudsen numbers $\epsilon = 1$ and $\epsilon = 0.01$, comparing with the implicit scheme for BGK model (S_i) at $t = 0.1$.

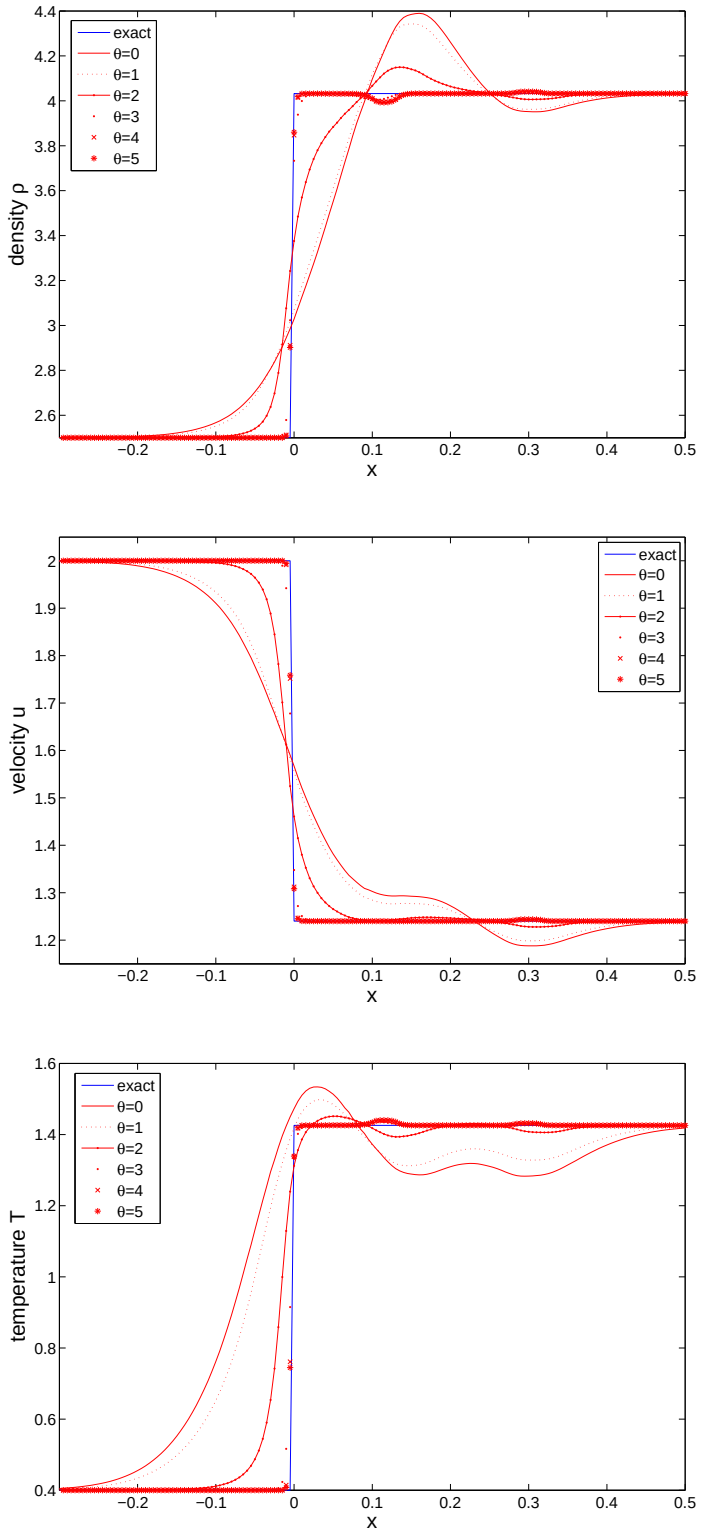

Figure 4: Stationary shock: the asymptotic properties of the scheme (MM) with different $\epsilon = 10^{-\theta}$ at $t = 0.1$. Profiles of mass density ρ on the top, mean velocity u in the middle, and mean temperature T on the bottom, as a function of space x.

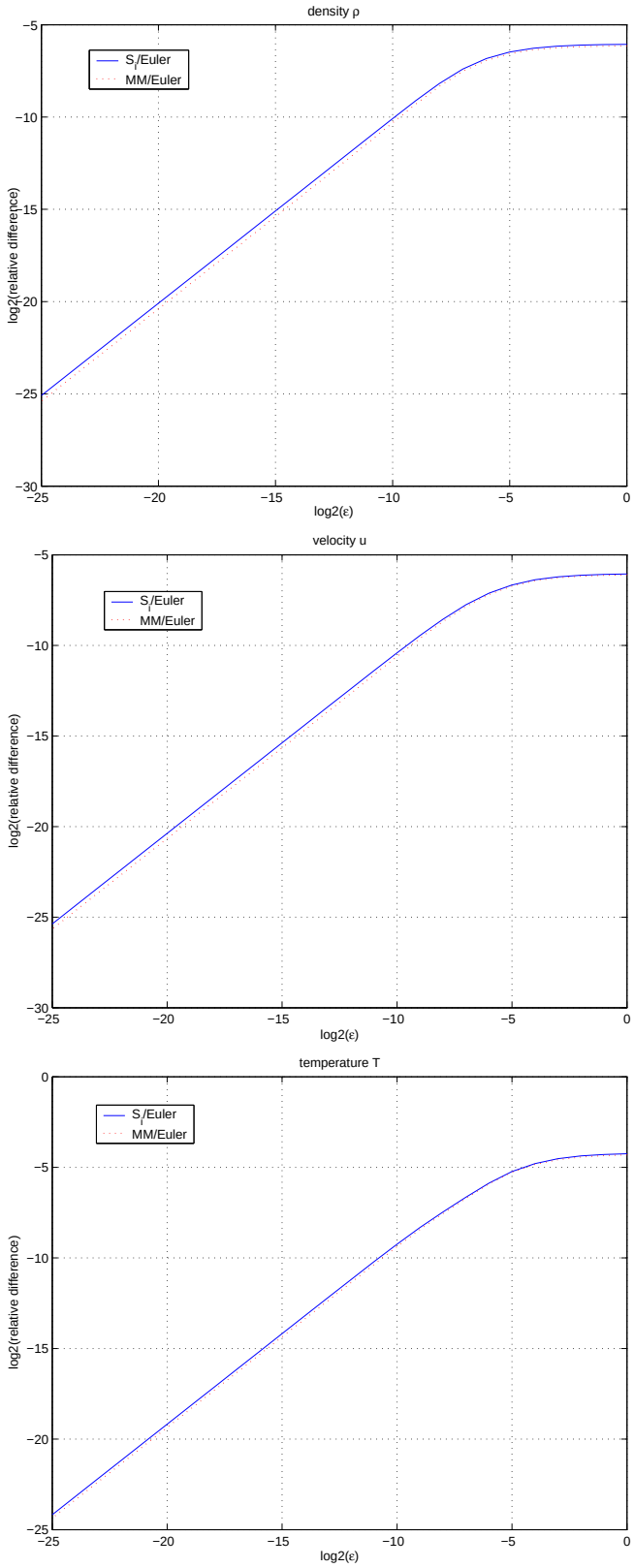

Figure 5: Stationary shock: the relative error between (MM) and (Euler), and between (S_i) and (Euler) for different $\epsilon = 2^{-\theta}, \theta = 0, 1, 2, 3, ..., 25$ at $t = 0.1$.

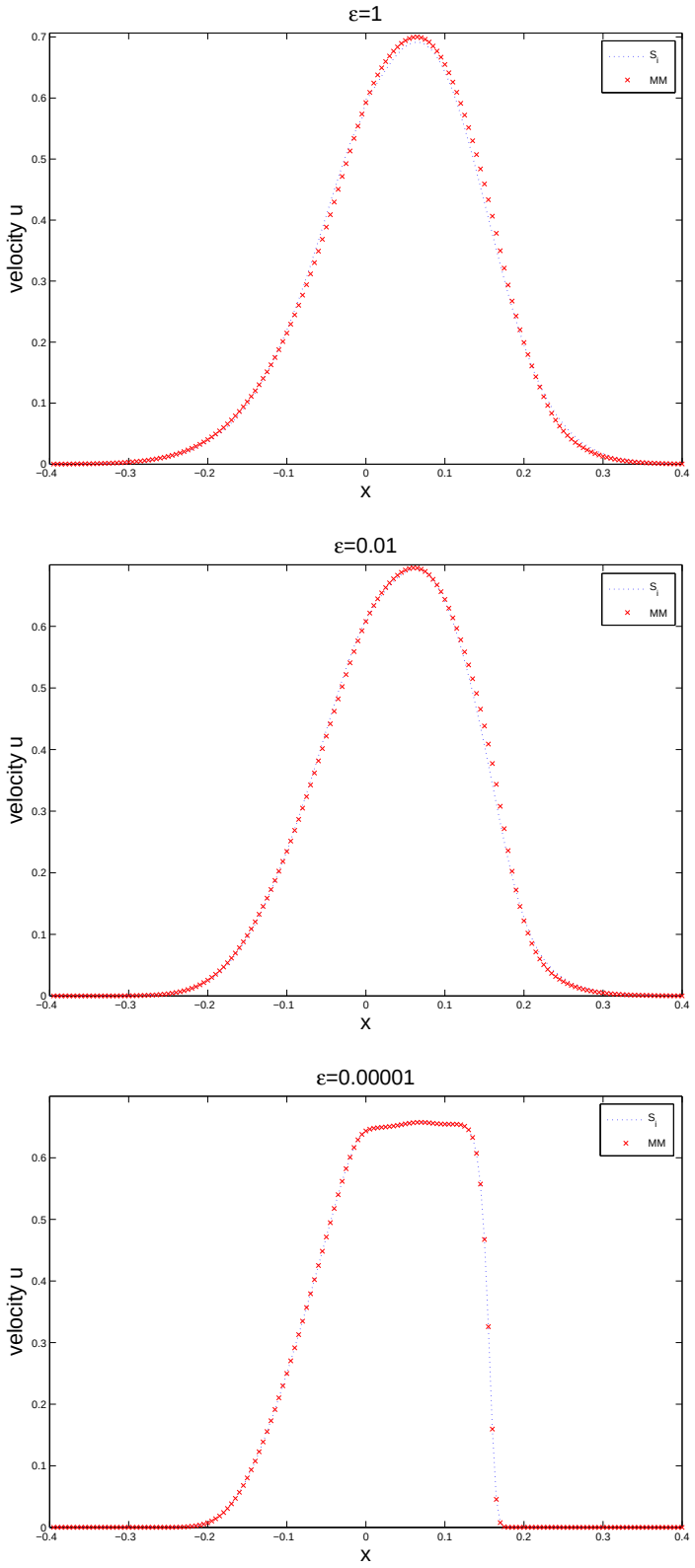

Figure 6: Sod problem: compare the mean velocity u given by the scheme (MM) with the implicit scheme S_i for the BGK model under different regimes: kinetic regime ($\epsilon = 1$), transition regime ($\epsilon = 10^{-2}$) and fluid regime ($\epsilon = 10^{-5}$) at $t = 0.1$.

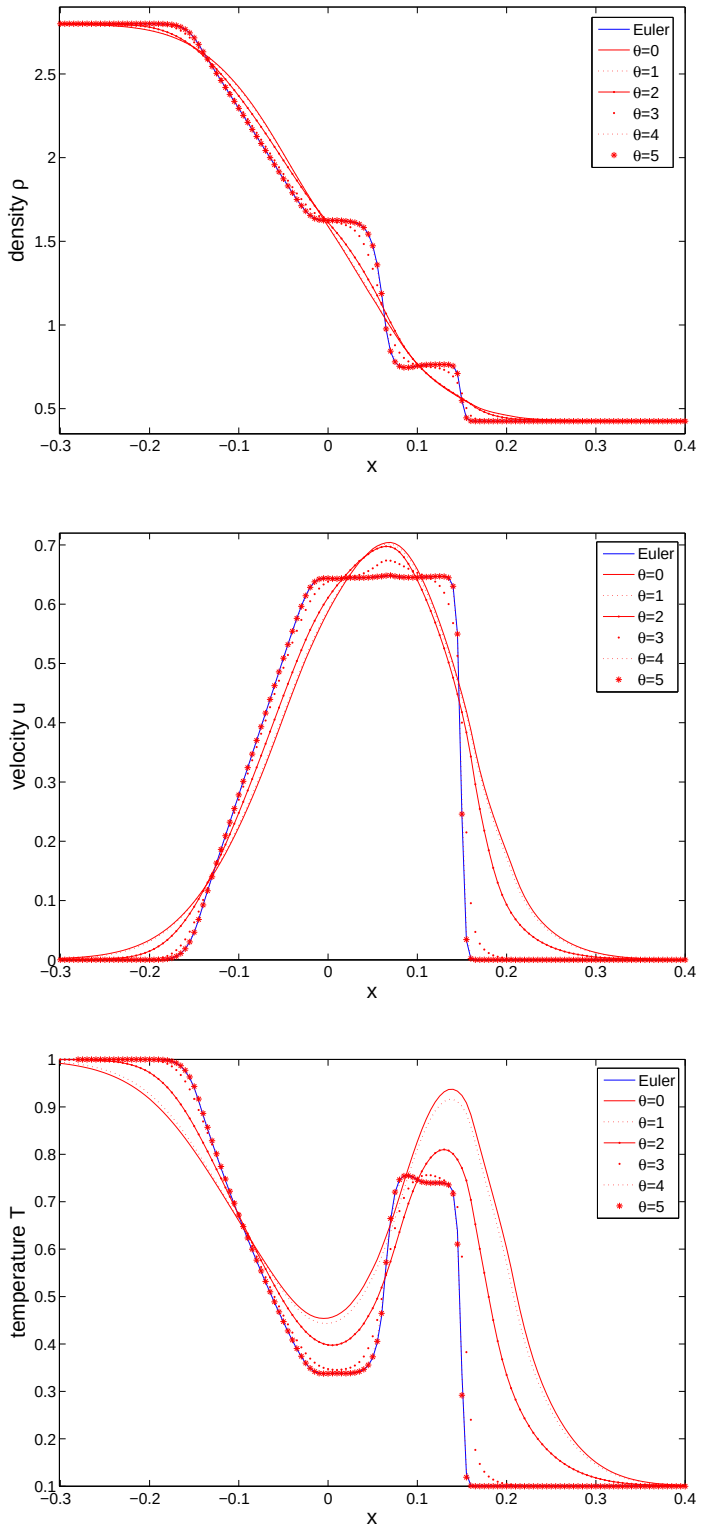

Figure 7: Sod problem: the asymptotic properties of the scheme (MM) with different $\epsilon = 10^{-\theta}$ at $t = 0.1$. Profiles of mass density ρ on the top, mean velocity u in the middle, and mean temperature T on the bottom, as a function of space x.

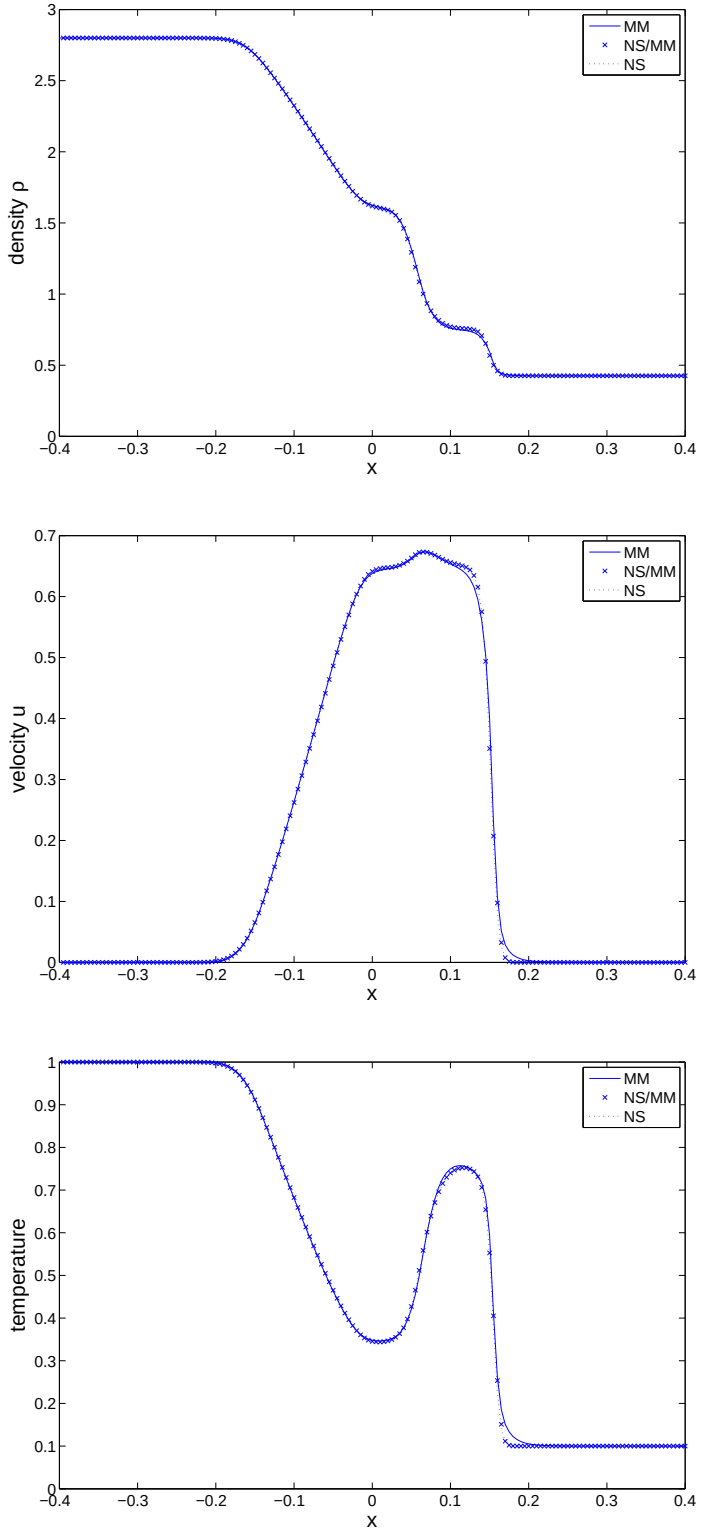

Figure 8: Sod problem: compare the schemes (MM), (NS) and (NS/MM) at $\epsilon = 0.001, \Delta x = 0.005, \frac{\Delta x}{\Delta t} = 100$ and $t = 0.1$.